Operating Temperatures and Diurnal Temperature Variations of Modules Installed in Open-Rack and Typical BIPV Configurations

Ebrar Özkalay, Gabi Friesen, Mauro Caccivio, Pierluigi Bonomo, Andrew Fairbrother, Christophe Ballif, and Alessandro Virtuani

***Abstract*—Because of the building skin integration with restricted rear-side ventilation, elevated operating temperatures are expected in building-integrated (BIPV) modules and systems, which may impact their long-performance and reliability. This work reports an analysis of operating temperatures and diurnal (day-night) temperature variations of the modules in open-rack and some BIPV mounting configurations (BIPV-ventilated and BIPV-insulated) monitored over a period of 2 to 5 years in southern Switzerland. The modules in BIPV configurations operated at 20 to 30˚C higher temperatures than the same modules installed in an open-rack configuration. In the worst-case, the temperature of the BIPV modules reached values slightly above 90˚C. In addition, the modules installed in BIPV configurations were confronted with considerably greater diurnal (day-night) temperature variations compared to the same modules with an open-rack mounting (on average 18 to 25˚C more). This demonstrates that these modules can suffer from higher thermo-mechanical stresses, potentially leading to accelerated degradation rates and shorter lifetimes. The suitability of the indoor qualification and safety tests in IEC 61215 and IEC 61730 were evaluated according to the threshold set at the 98th percentile real-life operating module temperature (as defined in the IEC TS 63126 guideline for qualifying PV modules operating at elevated temperatures). The study shows that according to IEC TS 63126, BIPV modules on a tilted surface in southern Switzerland may need to be tested at harsher environmental conditions (e.g., higher temperatures) in a selection of indoor qualification and safety tests.**

***Index Terms*—Building-integrated photovoltaics (BIPV), diurnal (day-night) temperature variation, IEC TS 63126, module temperature, T_{98}.**

This work was supported by the Swiss National Science Foundation under COST IZCOZ0_182967/1.

Ebrar Özkalay, Gabi Friesen, Mauro Caccivio, and Pierluigi Bonomo are with the Department for Environment Constructions and Design, University of Applied Sciences and Arts of Southern Switzerland (SUPSI), CH-6850 Mendrisio, Switzerland (e-mail: ebrar.ozkalay@supsi.ch; gabi.friesen@supsi.ch; mauro.caccivio@supsi.ch; pierluigi.bonomo@supsi.ch).

Andrew Fairbrother, Christophe Ballif, and Alessandro Virtuani are with the Photovoltaics and Thin Film Electronics Laboratory, Institute of Microengineering, École Polytechnique Fédérale de Lausanne (EPFL), 2000 Neuchâtel, Switzerland (e-mail: andrew.fairbrother@epfl.ch; christophe.ballif@epfl.ch; alessandro.virtuani@epfl.ch).

I. INTRODUCTION

BUILDING-INTEGRATED photovoltaics (BIPV) is one of the rapidly growing areas in photovoltaic (PV) applications in order to achieve nearly zero energy buildings and reduce greenhouse emissions [1]. As opposed to the majority of rooftop PV installations, where the modules are added on top of an existing building element, BIPV modules and systems are an integral part of the building envelope. BIPV elements are therefore "building active elements" replacing conventional parts of the building skin that generate electricity while simultaneously providing building envelope functions, such as weather protection (e.g. waterproofing, sunshade), thermal insulation, noise protection, daylight illumination or safety. The main difference between building applied PV (BAPV) and BIPV is the multi-functionality of BIPV besides electricity generation. The status of BIPV in Europe, relying on extensive BIPV case studies and products, is facing the implementation of cost reduction roadmaps addressing the whole BIPV value chain to support investors and real estate developers [2]. However, despite the growth and increasing attention on BIPV applications, several barriers and constraints still exist. Unlike conventional field installations, BIPV modules are generally installed with different orientations, which are often in non-optimal conditions. A common concern is the harsher operating conditions of BIPV modules relative to field installed PV, including 1) operating at higher temperatures due to reduced or restricted rear-side ventilation [3]–[5], 2) higher diurnal (day-night) temperature variations, and 3) periodic shading caused by surrounding buildings or other obstacles (will be treated in other publication). These are critical factors potentially impacting both the short-term and long-term performance of BIPV modules [6]–[8]. Elevated temperatures reduce the instantaneous power output of modules, and will accelerate the degradation of polymeric and other materials, and cause thermo-mechanical stresses due to variations in diurnal temperatures and mismatches in the thermal expansion coefficients of module materials [9]. A deeper understanding on the operating temperature of BIPV modules is critical in predicting these effects. Recently, the International Electrotechnical Commission (IEC) published a technical specification (TS) called IEC TS 63126 "Guidelines for qualifying PV modules, components and materials for operation at high temperatures" [10] as modules in hot

climates or in BIPV configurations may operate at temperatures higher than those used in the qualification and safety tests of IEC 61215 and IEC 61730 [11], [12]. The TS suggests that a module deployed under these specific conditions should be subjected to accelerated-aging tests at harsher conditions (e.g. increase in testing temperature or applied current). Testing conditions of a set of indoor qualification and safety tests (e.g. the upper-temperature limit of the thermal cycling test) depend on the 98th percentile operating module temperature (T_{98}) (Level 1 Test Condition for 70˚C < T_{98} ≤ 80˚C and Level 2 Test Condition for 80˚C < T_{98} ≤ 90˚C). T_{98} represents a cumulative exposure of 175.2 hours/year at or above the stated temperature. It is a combination of high temperature and time spent at high temperatures. The reference [13] summarizes the scientific background for T_{98}, the suggested changes to the qualification tests and the modelled operating module temperature for different mounting configurations and locations. Various studies have demonstrated measured or modelled operating temperature of PV modules in different climate conditions and mounting configurations [5], [14]–[16]. However, there is still a lack of detailed analysis on measured operating module temperature and T_{98} in BIPV mounting configurations (BIPV-ventilated and BIPV-insulated).

This work reports the operating temperatures including T_{98} and the diurnal temperature variations of modules in open-rack and BIPV configurations (BIPV-ventilated and BIPV-insulated) obtained from three BIPV outdoor test stands located on the premises of SUPSI in Canobbio, Switzerland. The suitability of the selected indoor qualification and safety tests in IEC 61215 and IEC 61730 are evaluated depending on T_{98} as defined in IEC TS 63126. This work is the enhanced version of the previous work on the operating temperature of the modules in open-rack and some BIPV configurations [17]. The diurnal (day-night) temperature variations of the modules in the open-rack and some BIPV mounting configurations are reported and discussed in addition to the previous work.

II. BIPV Test Stands

Three BIPV outdoor test stands were monitored at SUPSI in Canobbio, Switzerland, which according to Köppen-Geiger is classified as having a Cfb climate (temperate and humid climate, and warm summers) [18]. The modules on the test stands were installed in the open-rack and BIPV configurations as summarized in Fig. 1 and Table I.

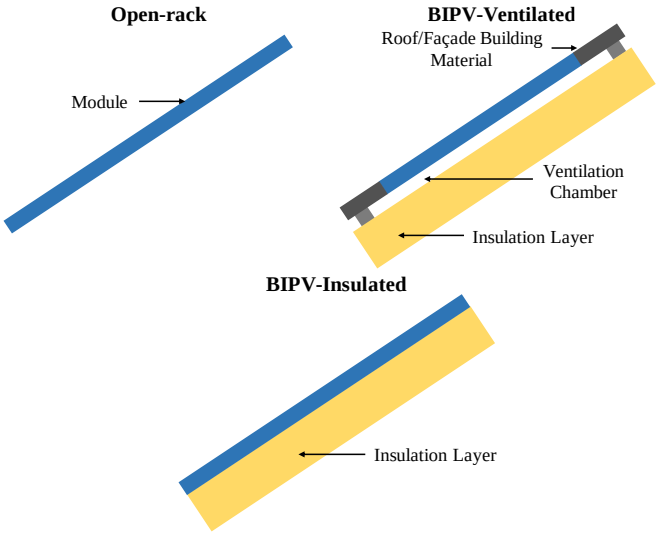

Fig. 1. Summary of installation configurations on the BIPV test stands.

Fig. 2 shows the probability density of the ambient temperature and the plane of array irradiances on the test stands. As expected, the maximum irradiance of the sloped surfaces were higher than the façade surface. There are two peaks on the irradiance profile of the vertical façade, which are in winter at about 810 W/m^2 and in summer at about 460 W/m^2.

The **open-rack** configuration, provisioned with full rear-side ventilation, is the most common and conventional PV module installation configuration used in ground-mounted and utility-scale PV systems. Due to free ventilation on the rear-side, open-rack modules are expected to operate at lower temperatures compared to BIPV modules. The most common BIPV solutions are in-roof solutions for discontinuous opaque roofing (cold ventilated roof) and opaque ventilated (cold-façade) for vertical surfaces [2]. These building skin solutions are conceived with a ventilation chamber behind the cladding, namely between the module and the insulation layer, which ensures partial ventilation on the rear-side of the module, as schematically represented in Fig. 1. The modules in this configuration are here referred to as **ventilated** or **BIPV-ventilated** modules. The other BIPV mounting configuration is characterized by a unitized cladding element without an air

TABLE I. Characteristics of the three Test Stands, including the modules used and the topology of installation. The thicknesses of the ventilation chambers for the modules in BIPV-ventilated configuration are stated in parentheses.

Test Stand	Cell and Module Technologies	Installation Configuration	Azimuth (South = 0˚) / Tilt Angles	Duration	Monitored Parameters
1	Al-BSF - G/EVA/BS Commercial module	• Open-rack • BIPV-Insulated	-4˚ / 6˚ (Roof)	51 Months	• G_{POA} (every 1 minute) • Module Temperature (Pt100 on rear-side of the modules) (every 1 minute) • Electrical performance using MPP tracker (every 1 minute)
	Al-BSF - G/PVB/G Commercial module				
2	HJT - G/G Prototype module	• Open-rack • BIPV-Ventilated (6 cm)	-4˚ / 20˚ (Roof)	53 Months	
	PERC - G/EVA/BS Commercial module	• BIPV-Ventilated (12 cm)			
3	PERC - G/PVB/G Commercial module	• BIPV-Ventilated (8 cm)	-4˚ / 90˚ (Façade)	27 Months	

Al-BSF: Aluminum back surface field, HJT: Heterojunction Technology, PERC: Passivated Emitter and Rear Contact, G: Glass, BS: Backsheet, EVA: Ethylene-vinyl acetate, PVB: Polyvinyl-butyral, G_{POA}: Plane of array irradiance and MPP: Maximum power point.

gap between the module and insulation layer. Hence, the rear-side ventilation is restricted. Both roofs and façades can be installed in a BIPV-insulated configuration, as typical of prefabricated building solutions. The modules in this configuration are here referred to as **insulated** or **BIPV-insulated** modules.

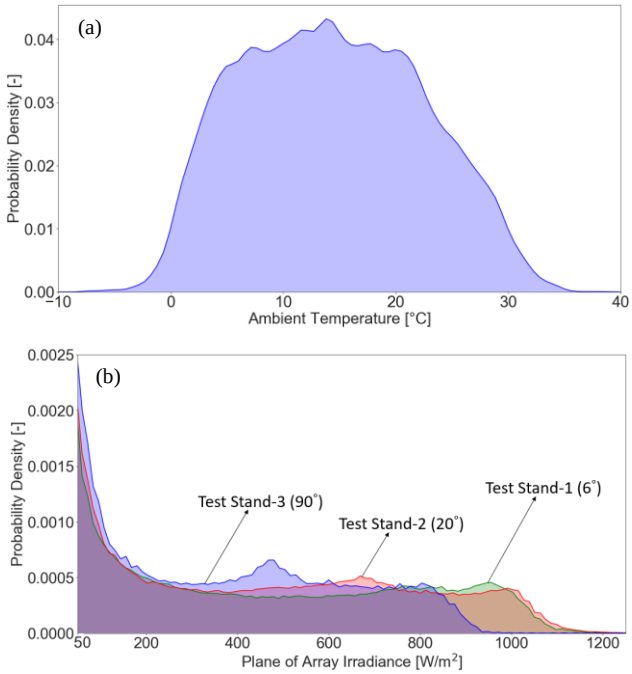

Fig. 2. Probability density of (a) ambient temperature and (b) plane of irradiances of the test stands for the measurement site. Only full-year data are used to prevent biases due to seasonal variations.

As shown in Table I, **Test Stand-1** consisted small-scale demonstrators representing discontinuous opaque ventilated roof of two module types, including aluminum back surface field (Al-BSF) glass/ethylene-vinyl acetate/backsheet (G/EVA/BS) and glass/polyvinyl-butyral/glass (G/PVB/G) modules. These were installed in open-rack and insulated configurations. The module performances and the related meteorological parameters were monitored for 51 months. The modules were installed at a tilt angle of 6˚ and azimuth of -4˚ from South. For the insulated configuration, 20 cm thick polyurethane foam was used, thus not allowing any rear-side ventilation.

Test Stand-2 consisted of small-scale demonstrators representing discontinuous opaque ventilated roof (about 6 m^2), with two module types: (1) heterojunction (HJT) solar cells in a glass/glass (G/G) configuration and (2) passivated emitter and rear contact (PERC) cells in a G/EVA/BS configuration. The HJT modules were installed in open-rack and roof ventilated configurations while the PERC module was installed only in ventilated configuration. The modules and the related meteorological parameters were monitored for 53 months. The ventilated HJT and PERC modules had 6 cm and 12 cm wide ventilation chamber to ensure building skin ventilation, respectively. The modules were installed at a tilt angle of 20˚ and azimuth of -4˚ from South. All the real roof construction skin was reproduced underneath.

In **Test Stand-3**, a PERC G/PVB/G module in a ventilated configuration at 90˚ tilt (resembling installation in an opaque façade) was monitored for 27 months. The ventilation chamber between the module and the insulation material was 8 cm wide. All the real façade construction skin was reproduced underneath.

The HJT modules on Test Stand-2 are prototype modules, while the other modules are commercial products. Each module was connected to a maximum power point tracker (MPPT3000) specially developed by SUPSI [19]. The hardware combines IV tracing performed every 5 minutes, while the module is otherwise operated at its maximum power using a maximum power point (MPP) tracker. In addition to the module's maximum power point current (I_{mp}) and voltage (V_{mp}) values delivered by the MPP tracker and the IV curves, the devices also acquire the plane of array irradiance (measured with a calibrated pyranometer) and the back of module temperature (measured with a Pt100 centered on the rear-side of the module). The temperature measurements were performed between 5:00 AM and 9:00 PM local time (Coordinated Universal Time+1 (UTC+1)). The effect of not having 24-hour temperature monitoring data is negligible on the operating temperature analysis since this work is focused on high operating temperatures and the reliability of the module materials. If we had 24-hour module temperature data, the operating module temperature ranges would be similar, but the time spent at the lower temperatures (due to the addition of nighttime data) would increase.

III. Results and Discussion

In this section, comparisons between the operating temperatures of the modules from the same and different test stands were performed. The comparisons that may be unreliable were avoided due to differences in design or module technologies (e.g. the absence of a module in open-rack configuration, the difference in the design of mounting configurations).

TABLE II. Maximum temperature (T_{MAX}) and T_{98} of the modules from Test Stand-1, Test Stand-2 and Test Stand-3. T_{98} values in bold are high enough to warrant harsher testing conditions for the related tests according to IEC TS 63126 [9]. Only full-year data used to prevent bias due to seasonal variation.

Test Stand	Cell and Module Technologies	Tilt Angles	Open-Rack		BIPV-Ventilated		BIPV-Insulated		Temperature Difference (BIPV – Open-rack)	
			T_{98} [˚C]	T_{max} [˚C]	T_{98} [˚C]	T_{max} [˚C]	T_{98} [˚C]	T_{max} [˚C]	T_{98} [˚C]	T_{max} [˚C]
1	Al-BSF - G/EVA/BS	6˚	57	66	-	-	**80**	92	23	26
	Al-BSF - G/PVB/G	6˚	53	62	-	-	**80**	91	27	29
2	HJT - G/G	20˚	50	64	**71**	83	-	-	21	19
	PERC - G/EVA/BS	20˚	-	-	63	77	-	-	-	-
3	PERC - G/PVB/G	90˚	-	-	59	68	-	-	-	-

A. Operating Module Temperature

Operating temperature distributions of the modules on the test stands for the duration of their monitoring periods are shown in Fig. 3 and summarized in Table II. T_{98} of each module was determined from the cumulative hours spent at temperatures since some of the nighttime temperature measurements (from 9:00 PM to 5:00 AM, UTC+1) were not recorded. One-minute temperature data series were sorted from highest to lowest module temperature, and T_{98} was determined by cumulative exposure of 175.2 hours/year. T_{98} values in Table II represents cumulative exposure of 175.2 hours/year at or above stated temperature. Only full-year data were used in Fig. 3 and for the calculation of T_{98} to avoid bias due to seasonal variation in temperature of the modules. For Test Stand-1, Test Stand-2, and Test Stand-3, the distribution corresponds, respectively, to 48, 48 and 24 months of data acquisition.

The insulated modules in **Test Stand-1** operated at higher temperatures due to absence of rear-side ventilation (Fig. 3a). While the open-rack modules reached a maximum of 62˚C and 66˚C, respectively, the insulated modules exhibited a larger distribution, reaching temperatures slightly above 90˚C. T_{98} of the insulated modules in Test Stand-1 are 80˚C, while T_{98} of the open-rack G/BS and G/G modules are 57˚C and 53˚C, respectively (Table II). Interestingly, the insulated modules are exposed to lower temperatures (even below 0˚C) with respect to modules in open-rack conditions. This is due to the stronger radiative cooling for the insulated modules compared to the open-rack modules at night. This behavior has been observed by others [16], [20].

There is a difference between the temperature distributions of the open-rack modules, whereas we observed no significant difference between the temperature distributions of the insulated modules (Fig. 3a). Open-rack modules dissipate heat on both sides by convective and radiative exchange with the sky/ground [21]. The open-rack G/G module ran cooler than the open-rack G/BS module. This is partly because the glass has 6% higher emissivity than the backsheet [22]. However, this difference in heat loss from the rear-side is negligible for the insulated modules since they were covered with 20 cm thick insulation material. Additionally, the module temperatures measured on the rear-side of the open-rack modules may not represent the actual cell temperatures due to the thermal gradient through the module materials and the heat capacitance of the module materials [23]. The estimated temperature difference between the cell and rear-side of the modules is about 1˚C and 2.2˚C for G/BS and G/G modules in open-rack, respectively [16], [24].

In **Test Stand-2**, the ventilated HJT module reached higher operating temperatures than the same module type in open-rack configuration due to limited rear-side ventilation (Fig. 3b). T_{98} of the open-rack and the ventilated HJT modules are 50˚C and 71˚C, respectively (Table II). The ventilated PERC module has a T_{98} of 63˚C (maximum of 77˚C). In the ventilated roof configuration, the HJT module operated warmer than the PERC module, which could be due to difference in the design of the ventilation systems (e.g. different ventilation chamber thicknesses and techniques, and ventilation outlet positions), the position of the module within the roof surface and parasitic absorption by transparent conductive oxide (TCO) layer of the HJT cells [25].

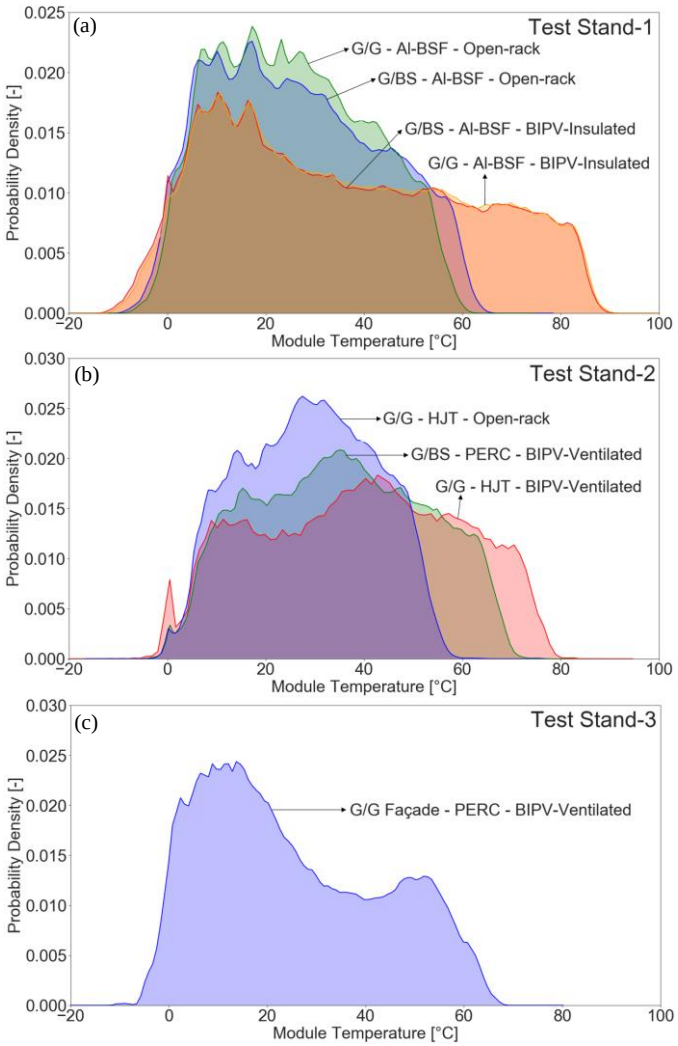

Fig. 3. Temperature distribution of the modules at (a) Test Stand-1, (b) Test Stand-2 and (c) Test Stand-3 obtained from temperature measurements made between 5:00 AM and 9:00 PM local time (UTC+1). Only full-year data are used to prevent biases due to seasonal variations in module temperature. For Test Stand-1, Test Stand-2, and Test Stand-3 the distribution corresponds, respectively, to 48, 48 and 24 months of data acquisition. For each module, the integral of the temperature distribution corresponds to one.

The ventilated G/G PERC BIPV module, installed as a ventilated façade module on **Test Stand-3**, operated at lower temperatures as compared to the other modules in BIPV configurations (Fig. 3c). As expected, this is due to the fact that façades received a higher insolation in winter months (e.g. when the sun is lower on the horizon, and average temperatures are lower) with respect to summer months. On the contrary, the modules on a sloped surface generally reach their maximum operating temperatures in summer when solar altitude and ambient temperatures are high.

The operating temperatures of the sloped roof modules have a seasonality that is high in summer (high ambient temperature and G_{POA}) and low in winter (low ambient temperature and G_{POA}) on average. Unlike the sloped roof modules, the façade module was exposed to high ambient temperature and low G_{POA} in summer and low ambient temperature and high G_{POA}

in winter. Due to the mismatch between ambient temperature and G_{POA} of the façade, the temperature of the façade module does not have a strong seasonality like the sloped roof modules. In contrast to the sloped roof modules, the façade module has two clear peaks at about 10˚C and about 50˚C (Fig. 3c). The first peak at about 10˚C is due to overcast days throughout the year. The second peak at about 50˚C is due to clear sky days throughout the year.

T_{98} of the two insulated BIPV modules on Test Stand-1 and the ventilated HJT module on Test Stand-2 are all higher than 70˚C, as shown in Table II. According to the IEC TS 63126, these modules should be tested at harsher testing conditions (Level 1 Test Condition) in a selection of indoor module qualification and safety tests defined in IEC 61215 and IEC 61730.

B. Diurnal (Day-Night) Module Temperature Variation

Diurnal (Day-Night) temperature variations (ΔT_D) of the modules were calculated from the difference between each module's maximum and minimum temperatures in 24 hours. Missing nighttime temperature monitoring before 5:00 AM (UTC+1) usually does not have a significant impact for the ΔT_D analysis since the coldest time of a day is generally between 5:00 AM (UTC+1) and sunrise for Canobbio, Switzerland. The ΔT_D distributions of the modules are shown in Fig. 4 and summarized in Table III. In the ΔT_D analysis, full-year data were used to prevent bias due to seasonal variation in module temperature. For Test Stand-1, Test Stand-2, and Test Stand-3, the distribution corresponds, respectively, to 48, 48 and 24 months of data acquisition.

The slight increase in the probability density of ΔT_D below 15˚C is due to overcast and cloudy days. For cloudy days, the median of ΔT_D distributions ($\Delta T_{D,median}$) of the modules are between 10 to 13˚C, and there is no significant difference between the modules since the amount of received irradiance is low. The higher probability densities of ΔT_D above 20˚C represent clear sky days. Depending on the various parameters (e.g. mounting configuration, module technology, inclination), the peak of ΔT_D distribution differs between the modules (Fig. 4).

In **Test Stand-1**, the $\Delta T_{D,median}$ of the open-rack modules are around 26 to 30˚C, while the $\Delta T_{D,median}$ of the insulated modules are around 50 to 51˚C (Table III). For the G/G modules, the $\Delta T_{D,median}$ of the insulated module (51˚C) is almost twice as the $\Delta T_{D,median}$ of the open-rack module (26˚C). The maximum ΔT ($\Delta T_{D,max}$) for the insulated modules reached 76 to 77˚C, while for the open-rack modules, it was never above 50˚C. There is almost no difference between the insulated G/G and G/BS modules but the open-rack G/BS module was exposed to larger ΔT_D compared to the open-rack G/G module (Fig. 4a). This is because the open-rack G/G module operated slightly warmer than the open-rack G/BS module.

In **Test Stand-2**, although the $\Delta T_{D,median}$ of the open-rack HJT module is 26˚C, the ventilated HJT module has the median at 44˚C (Table III). The $\Delta T_{D,max}$ of the ventilated HJT and PERC roof modules are 66˚C and 58˚C, respectively. Since the ventilated HJT BIPV module ran warmer than the ventilated PERC BIPV module, it was exposed to greater ΔT_D.

The insulated G/G BIPV module on Test Stand-1 was exhibited a greater ΔT_D compared to the ventilated G/G HJT BIPV module on Test Stand-2 (Fig. 4a and Fig. 4b). This is mainly because the insulated configuration has no rear-side ventilation, whereas the ventilated configuration has limited rear-side ventilation. The insulated G/G and ventilated G/G HJT BIPV modules have 25˚C and 18˚C greater $\Delta T_{D,median}$ with respect to their pairs in the open-rack configuration, respectively.

As shown in Table II, there is no significant difference between the T_{98} and the maximum temperatures of the open-rack modules (Test Stand-1 and Test Stand-2) and the ventilated façade module on **Test Stand-3**. On the other hand, the façade module experienced higher ΔT_D than the open-rack modules (Fig. 4). The $\Delta T_{D,median}$ of the ventilated façade module on Test Stand-3 is 43˚C, which is well above the $\Delta T_{D,median}$ of any open-rack module (13 to 17˚C more) as shown in Table III.

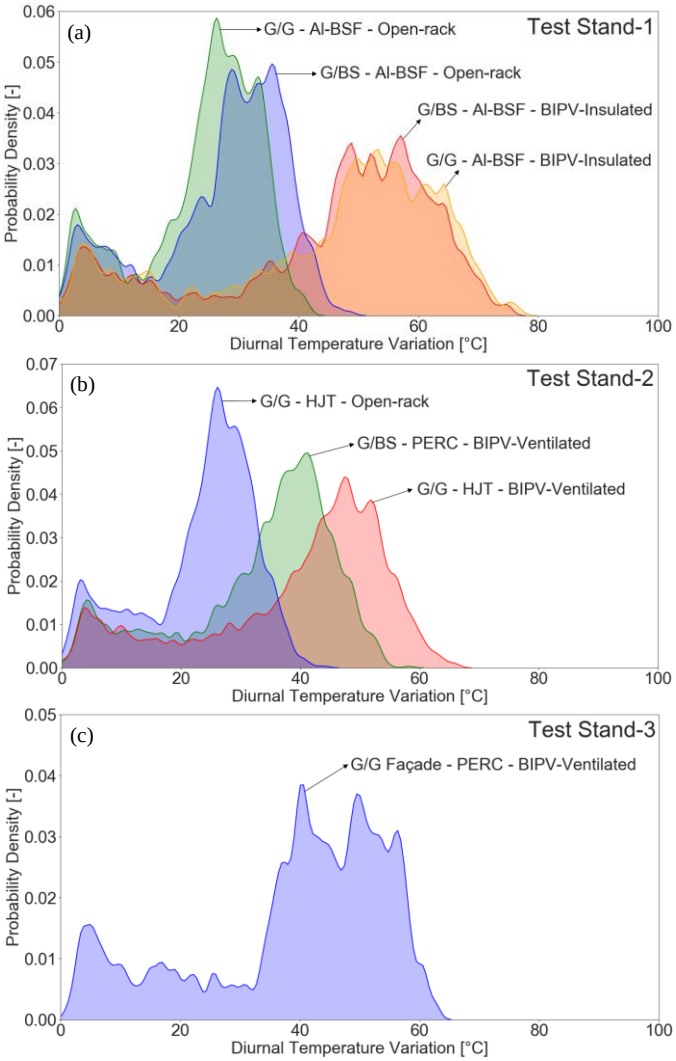

Fig. 4. Diurnal temperature variation distribution of the modules at (a) Test Stand-1, (b) Test Stand-2 and (c) Test Stand-3 obtained from temperature measurements made between 5:00 AM and 9:00 PM local time (UTC+1). Only full-year data used to prevent bias due to seasonal variation. For Test Stand-1, Test Stand-2, and Test Stand-3 the distribution corresponds, respectively, to 48, 48 and 24 months of data acquisition. For each module, the integral of the distribution corresponds to one.

TABLE III. MEDIAN ($\Delta T_{D,MEDIAN}$) AND MAXIMUM ($\Delta T_{D,MAX}$) DIURNAL TEMPERATURE VARIATIONS OF THE MODULES FROM TEST STAND-1, TEST STAND-2 AND TEST STAND-3. ONLY FULL-YEAR DATA IS USED TO PREVENT ANY BIAS DUE TO SEASONAL VARIATIONS OF MODULE TEMPERATURE.

Test Stand	Cell and Module Technologies	Tilt Angles	Open-Rack		BIPV-Ventilated		BIPV-Insulated		Difference (BIPV – Open-rack)	
			$\Delta T_{D,median}$ [°C]	$\Delta T_{D,max}$ [°C]	$\Delta T_{D,median}$ [°C]	$\Delta T_{D,max}$ [°C]	$\Delta T_{D,median}$ [°C]	$\Delta T_{D,max}$ [°C]	$\Delta T_{D,median}$ [°C]	$\Delta T_{D,max}$ [°C]
1	Al-BSF - G/EVA/BS	6°	30	49	-	-	50	76	**20**	**27**
	Al-BSF - G/PVB/G	6°	26	42	-	-	51	77	**25**	**35**
2	HJT - G/G	20°	26	44	44	66	-	-	**18**	**22**
	PERC - G/EVA/BS	20°	-	-	37	58	-	-	-	-
3	PERC - G/PVB/G	90°	-	-	43	63	-	-	-	-

Fig. 5 shows the plane of array irradiances and module temperatures from Test Stand-2 and Test Stand-3 on December 24, 2017, the closest clear sky day to the winter solstice. When the sun is low on the horizon, the vertical façade module on Test Stand-3 has higher operating temperatures (Fig. 5b) than the 20°-tilted roof modules on Test Stand-2, due to the higher amount of irradiance received (Fig. 5a). Hence, the façade BIPV module has higher ΔT_D (59°C) with respect to the other modules (maximum of 49°C). The façade module experienced the $\Delta T_{D,max}$ in clear-sky days when the solar altitude was low compared to June, and the nighttime temperatures were frequently below 5°C, especially around late February, March and early April for Canobbio. The sloped modules experienced the $\Delta T_{D,max}$ in clear-sky days when the differences between day and night ambient temperatures were high (>13°C), and the solar altitude was higher compared to December, especially around late March, April, late August and September for Canobbio. The time of the year with the $\Delta T_{D,max}$ could slightly vary depending on the tilt of the sloped modules.

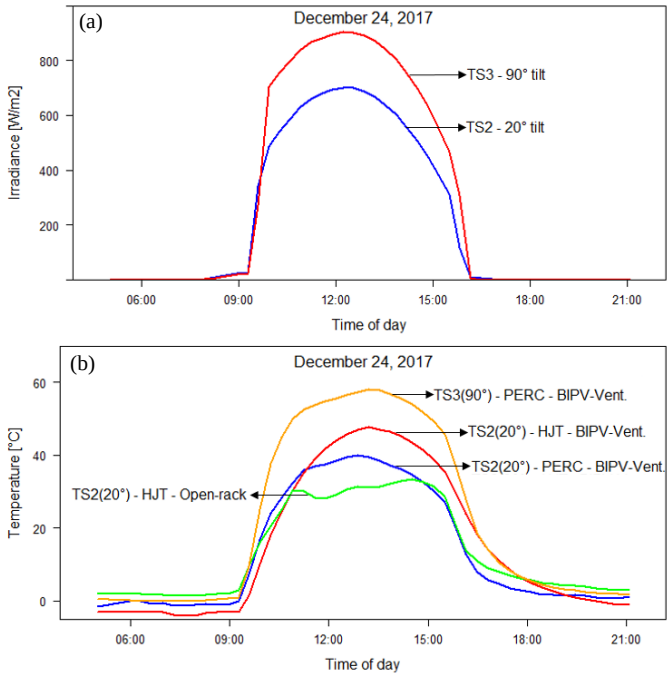

Fig. 5. Daily (a) plane of array irradiance and (b) module temperature profiles from Test Stand-2 (TS2) (20° tilt) and Test Stand-3 (TS3) (90° tilt) on December 24, 2017, the closest clear sky day to the winter solstice. All times are local time (UTC+1).

C. Impact of Temperature on Module Reliability

Table II shows that the BIPV modules installed in a mid-latitude country (Switzerland) with a reduced or restricted rear-side ventilation operated at temperatures 20 to 30°C higher than the same modules installed in an open-rack configuration. As shown in various studies [26]–[28], exposure of the modules to elevated operating temperatures may lead to higher degradation rates (e.g. higher rate of encapsulant discoloration, damaged interconnections and solder joints, etc.) and a faster occurrence of wear-out-failures that shorten the lifetime of a PV module.

Even in a vertical façade, BIPV modules were exposed to larger ΔT_D than the corresponding modules mounted in an open rack configuration. Larger temperature changes increase thermo-mechanical stresses on interconnects and cells due mismatches in the thermal expansion coefficients of the different materials used in the module sandwich [9]. Modules exposed to larger thermo-mechanical stresses may more easily be prone to larger failure rates of solder joints, interconnects or cells.

Over an extended time period, these degradation mechanisms may cause current mismatches between cells (evolving in other defects and in the worst case leading to hot-spot generation), increase in module's series resistance, and eventually in loss of power [29]. Various studies [30], [31] have demonstrated that modules in hot climates are subject to larger power losses due to increased series resistance compared to modules in cold climates. Increased series resistance could be one of the possible mechanisms for larger degradation rates of the modules operating at elevated temperatures. Furthermore, cell and metallization defects could cause hot spot and enhance occurrence of other failure modes such as discoloration, glass breakage and loss of electrical insulation.

Due to the exposure to higher operating temperatures, diurnal temperature changes, and proximity to end-users in buildings, BIPV modules should satisfy stricter safety and performance requirements (IEC TS 63126, IEC 63092-1 [32], IEC 63092-2 [33] and other regional and national standards specific to building materials), which can lead to modifications of the qualification and safety indoor tests.

IV. Conclusion

This work shows the operating temperatures of the modules in open-rack and BIPV mounting configurations during their monitoring of several years. Their operating temperatures including, T_{98} and diurnal (day-night) temperature variations depending on their mounting configurations, are compared. The maximum operating temperature of the insulated BIPV modules reached slightly above 90˚C in southern Switzerland. These modules have around 23 to 27˚C larger T_{98} compared to the same modules in open-rack due to restricted rear-side air ventilation. Similarly, the ventilated BIPV modules operated at higher temperatures than the open-rack modules (21˚C higher T_{98}). Furthermore, all BIPV modules, including the façade module, were exposed to greater diurnal (day-night) temperature variations with respect to the open-rack modules. In the worst-case situation, the insulated modules on a tilted surface experienced more than 75˚C temperature change, while the open-rack modules never experienced temperature changes greater than 50˚C between day and night.

The BIPV modules on a sloped roof surface were therefore exposed to larger thermal and thermo-mechanical stresses than the modules in a conventional open-rack configuration. These stresses could presumably accelerate the degradation of the polymeric materials in the module sandwich and cause damage to cells and metallic contacts. This could later cause higher degradation rates and shorten the lifetime of BIPV modules which calls for further investigation. According to IEC TS 63126, two insulated Al-BSF and the ventilated HJT BIPV modules ($70˚C < T_{98} \leq 80˚C$) operated at temperatures above the typical temperature ranges used in the qualification and safety tests of IEC 61215 and IEC 61730. Hence, for the selected modules, the qualification and safety tests should be performed at harsher testing conditions as defined IEC TS 63126.

Interestingly, the ventilated façade module ($\Delta T_{D,median}$ = 43˚C) experienced larger diurnal temperature changes with respect to the open-rack modules ($\Delta T_{D,median}$ = 26 to 30˚C), even though the façade module and the open-rack modules do not have significantly different T_{98} values and operating temperature ranges. This additional thermo-mechanical stress of the façade module compared to the open-rack modules may increase the risk of damage to metallic contacts, solder joints and cells. The long-term performance of the modules in this work and the effect of the elevated operating temperatures on them will be investigated as a follow-up work.

Acknowledgment

This work was supported in part by the Swiss National Science Foundation under COST IZCOZ0_182967/1. The authors would like to thank the University of Applied Sciences and Arts of Southern Switzerland (SUPSI) PVLab and BIPV-Innovative Building Skin Team researchers, and personnel, which contributed with data of the roof and façade BIPV facilities.

References

[1] G. Y. Palacios-Jaimes, P. Martn-Ramos, F. J. Rey-Martnez and I. A. Fernández-Coppel, "Transformation of a university lecture hall in Valladolid (Spain) into NZEB: LCA of a BIPV system integrated in its façade," *Int. J. Photoenergy*, pp. 1-11, 2017.

[2] P. Corti, P. Bonomo, F. Frontini, P. Mace and E. Bosch, "Building Integrated Photovoltaics: A practical handbook for solar buildings," 2020.

[3] T. Nordmann and L. Clavadetscher, "Understanding temperature effects on PV system performance," in *World Conf. on Photovolt. Energy Conv.*, 2003, pp. 2243-2246.

[4] A. Virtuani and T. Sample, "Modification to the standard reference environment (SRE) for nominal operating cell temperature (NOCT) to account for building integration," in *24th Eur. Photovolt. Sol. Energy Conf. Exhib.*, Hamburg, pp. 3332-3337, 2009.

[5] M. D. Kempe, D. C. Miller, J. H. Wohlgemuth, S. R. Kurtz, J. M. Moseley, Q. A. Shah, G. Tamizhmani, K. Sakurai, M. Inoue, A. Masuda, S. L. Samuels and C. E. Vanderpan, "Field testing of thermoplastic encapsulants in high-temperature installations," *Energy Sci. Eng.*, vol. 3, pp. 565-580, 2015.

[6] D. C. Jordan, C. Deline, M. Deceglie, T. J. Silverman and W. Luo, "PV degradation – mounting & temperature," in *Proc. IEEE 46th Photovolt. Spec. Conf.*, Chicago, 2019, pp. 673-679, doi: 10.1109/PVSC40753.2019.8980767.

[7] A. Gok, E. Ozkalay, G. Friesen and F. Frontini, "The influence of operating temperature on the performance of BIPV modules," *IEEE Journal of Photovoltaics*, vol. 10, no. 5, pp. 1371-1378, Sept. 2020, doi: 10.1109/JPHOTOV.2020.3001181.

[8] A. Virtuani and D. Strepparava, "Modelling the performance of amorphous and crystalline silicon in different typologies of building-integrated photovoltaic (BIPV) conditions," *Solar Energy*, vol. 146, pp. 113-118, 2017.

[9] N. Bosco, T. J. Silverman and S. Kurtz, "Climate specific thermomechanical fatigue of flat plate photovoltaic module solder joints," *Microelectronics Reliability*, vol. 62, pp. 124-129, 2016.

[10] IEC, "IEC TS 63126:2020 ED1 Guidelines for qualifying PV modules, components and materials for operation at high temperatures," International Electrotechnical Commission, 2020.

[11] IEC, "IEC 61215-2:2021 Terrestrial photovoltaic (PV) modules - Design qualification and type approval - Part 2: Test procedures," International Electrotechnical Commission, 2021.

[12] IEC, "IEC 61730-2:2016 Photovoltaic (PV) module safety qualification - Part 2: Requirements for testing," International Electrotechnical Commission, 2016.

[13] D. M. Kempe, D. Holsapple, K. Whitfield and N. Shiradkar, "Standards development for modules in high temperature micro-environments," *Progress in Photovoltaics: Research and Applications*, vol. 29, no. 4, pp. 445-460, 2021.

[14] M. D. Kempe, D. C. Miller, J. H. Wohlgemuth, S. R. Kurtz, J. M. Moseley, Q. Shah, G. Tamizhmani, K. Sakurai, M. Inoue, T. Doi, A. Masuda, S. L. Samuels and C. E. Vanderpan, "A field evaluation of the potential for creep in thermoplastic encapsulant materials," in *Proc. IEEE 38th Photovolt. Spec. Conf.*, 2012, pp. 1871-1876, doi: 10.1109/PVSC.2012.6317958.

[15] S. Kurtz, K. Whitfield, J. Joyce, J. Wohlgemuth, M. Kempe, N. Dhere, N. Bosco and T. Zgonena, "Evaluation of high-temperature exposure of rack-mounted photovoltaic modules," in *Conference Record of the IEEE Photovoltaic Specialists Conference*, 2009, pp. 2399-2404, doi: 10.1109/PVSC.2009.5411307.

[16] A. Fairbrother, A. Virtuani and C. Ballif, "Outdoor operating temperature of modules in BIPV and BAPV topologies," in *37th Eur. Photovolt. Sol. Energy Conf. Exhib.*, 2020, pp. 1752-1756.

[17] E. Ozkalay, G. Friesen, A. Fairbrother, C. Ballif and A. Virtuani, "Monitoring of the operating Temperature of modules in open-rack and typical BIPV configurations," in *Proc. IEEE 48th Photovolt. Spec. Conf.*, 2021.

[18] M. Kottek, J. Grieser, C. Beck, B. Rudolf and F. Rubel, "World map of

the Köppen-Geiger climate classification," *Meteorologische Zeitschrift*, vol. 15, no. 3, pp. 259-263, 2006.

[19] D. Chianese, E. Burà and A. Realini, "MPPT3000 multifunction testing device for PV modules," in *24th Eur. Photovolt. Sol. Energy Conf. Exhib.*, Valencia, 2008, pp.3037-3040.

[20] M. Koehl, S. Hamperl and M. Heck, "Effect of thermal insulation of the back side of PV modules on the module temperature," *Progress in Photovoltaics: Research and Applications*, vol. 24, no. 9, pp. 1194-1199, 2016.

[21] G. Ciulla, V. Lo Brano and E. Moreci, "Forecasting the Cell Temperature of PV Modules with an Adaptive System", *Int. J. of Photoenergy*, 2013.

[22] M.W.P.E. Lamers, E. Özkalay, R.S.R. Gali, G.J.M. Janssen, A.W. Weeber, I.G. Romijn and B.B. Van Aken, "Temperature effects of bifacial modules: Hotter or cooler? ", *Solar Energy Materials and Solar Cells*, vol. 185, pp. 192-197, 2018, doi: 10.1016/j.solmat.2018.05.033.

[23] D. King, J. Kratochvil and W. Boyson, "Temperature coefficients for PV modules and arrays: measurement methods, difficulties, and results," in *Conference Record of the Twenty Sixth IEEE Photovoltaic Specialists Conference - 1997*, 1997, pp. 1183-1186, doi: 10.1109/PVSC.1997.654300.

[24] S. Krauter and A. Preiss, "Comparison of module temperature measurement methods," *2009 34th IEEE Photovolt. Spec. Conf.*, 2009, pp. 333-338, doi: 10.1109/PVSC.2009.5411669.

[25] Z. C. Holma, A. Descoeudres, L. Barraud, F. Z. Fernandez, J. P. Seif, S. De Wolf and C. Ballif, "Current losses at the front of silicon heterojunction solar cells," *IEEE Journal of Photovoltaics*, pp. 7-15, 2012.

[26] D. Jordan, S. Kurtz, K. VanSant and J. Newmiller, "Compendium of photovoltaic degradation rates," *Progress in Photovoltaics: Research and Applications*, no. 24, pp. 978-989, 2016.

[27] H. Hu, W. Gambogi, K. R. Choudhury, L. Garreau-Iles, T. Felder, S. MacMaster, O. Fu and T.-J. Trout, "Field analysis and degradation of modules and components in distributed PV applications," in *35th Eur. Photovolt. Sol. Energy Conf. Exhib.*, 2018, pp. 1072-1075.

[28] D. Rajiv, S. Chattopadhyay, V. Kuthanazhi, J. John, C. S. Solanki, J. M. Vasi, A. Kumar and O. S. Sastry, "Performance degradation in field-aged crystalline silicon PV modules in different Indian climatic conditions," in *Proc. IEEE 46th Photovolt. Spec. Conf.*, Denver, 2014, pp. 3182-3187, doi: 10.1109/PVSC.2014.6925612.

[29] A. Gok, E. Ozkalay, G. Friesen and F. Frontini, "Power loss modes of building-integrated photovoltaic modules: An analytical approach using outdoor I-V curves," *IEEE Journal of Photovoltaics*, vol. 11, no. 3, pp. 789-796, May 2021, doi: 10.1109/JPHOTOV.2021.3060719.

[30] D. C. Jordan, J. Wohlgemuth and S. Kurtz, "Technology and climate trends in PV module degradation," in *37th Eur. Photovolt. Sol. Energy Conf. Exhib.*, 2012, pp. 3118-3124.

[31] R. Dubey, S. Chattopadhyay, V. Kuthanazhi, J. John, B. M. Arora, A. Kottantharayil, K. L. Narasimhan, C. S. Solanki, V. Kuber and J. Vasi, "All-India Survey of Photovoltaic Module Degradation: 2013," National Centre for Photovoltaic Research and Education Indian Institute of Technology Bombay National Institute of Solar Energy, 2013.

[32] IEC, "IEC 63092-1:2020 Photovoltaics in buildings - Part 1: Requirements for building-integrated photovoltaic modules," International Electrotechnical Commission, 2020.

[33] IEC, "IEC 63092-2:2020 Photovoltaics in buildings - Part 2: Requirements for building-integrated photovoltaic systems," International Electrotechnical Commission, 2020.